

Enhancement of Temozolomide Cytotoxicity against Human Glioblastoma by Silver and Titanium Nanoparticles

Sakshi Goswami, Yeshvandra Verma and S V S Rana*

Department of Toxicology, Ch. Charan Singh University, Meerut, India

*Corresponding Author: S V S Rana, Professor Emeritus, Department of Toxicology, Ch Charan Singh University, Meerut, India.

Received: July 30, 2024; Published: September 13, 2024

Abstract

Temozolomide (TMZ), an antineoplastic drug, is the first line chemotherapeutic agent approved by FDA to treat human glioblastoma (GBM), a malignant tumor of central nervous system. However, a strategy of combined treatment of TMZ and nanoparticles has emerged as a novel approach to treat GBM. During present investigations, combined effects of TMZ, silver and titanium nanoparticles have been studied on GBM employing cytotoxicity parameters. Nanoparticles were characterized using a couple of methods. IC_{50} values of these agents were calculated following OECD guidelines. Human GBM cell line - U87MG were cultured under laboratory conditions. The cell were separated into different groups and exposed to different concentrations ranging from 200 μ M - 600 μ M of AgNPs, 12.5 μ M - 100.12 μ M of TiO_2 NPs and 200 μ M - 600 μ M of TMZ with MEM for 24h at 37°C and 5% CO_2 atmosphere. Thereafter, cytotoxicity amongst different groups of GBM was monitored through - trypan blue exclusion method, MTT assay and cell proliferation assay. The results showed a dose dependent effect of TMZ on cell mortality. Cytotoxicity was enhanced by combined treatments of TMZ and NPs. However, better effects were registered in GBM treated with TMZ+AgNPs than TMZ+ TiO_2 NPs. The cytotoxic effect has been attributed to reactive oxygen species generated by NPs. Further, the roles of enhanced permeability and retention (EPR) mechanism and nanoparticle induced epithelial cell leakiness (NanoEL) have also been discussed. In brief, present study suggests that a strategy of combined treatment with TMZ and NPs yields better antitumor results.

Keywords: Temozolomide; Glioblastoma; Silver Nanoparticles; Titanium Nanoparticles; Cytotoxicity

Abbreviations

GBM: Glioblastoma; TMZ: Temozolomide; PCV: Procarbazine, Lomustine and Vincristine; BBB: Blood Brain Barrier; NPs: Nanoparticles; AgNPs: Silver Nanoparticles; TiO_2 NPs: Titanium Dioxide Nanoparticles; MTT: 3-(4,5-Dimethylthiazol-2-yl)-2,5 Diphenyl Tetrazolium Bromide; FBS: Fetal Bovine Serum; NEAA: Non Essential Amino Acid; MEM: Minimum Essential Medium; ATCC: American Type Culture Collection; HRTEM: High Resolution Transmission Electron Microscopy; FESEM: Field Emission Scanning Electron Microscopy; EDAX: Energy Dispersive X-Ray Analysis; XRD: X-Ray Diffraction; SAIF: Sophisticated Analytical Instrumentation Facility; CIL: Central Instrumentation Facility; FTIR: Fourier Transform Infra Red Spectroscopy; IC_{50} : Half Maximal Inhibitory Concentration; PBS: Phosphate Buffered Saline; ANOVA: Analysis of Variance; DMSO: Dimethyl Sulfoxide; OD: Optical Density; NADPH: Nicotinamide Adenine Dinucleotide Phosphate Hydrogen; MTIC: 5-(3-Methyl-1-Triazeno) Imidazole-4-Carboxamide; MGMT: O⁶-Methylguanine-DNA-Methyltransferase; EPR: Enhanced Permeability and Retention; ROS: Reactive Oxygen Species; NanoEL: Nanomaterial Induced Endothelial Cells Leakiness

Introduction

Glioblastoma multiforme (GBM) is one of the most common malignant tumors of the central nervous system. GBM (anaplastic astrocytoma) is considered as a heterogeneous disease and factors viz. tumor cell origin, tumor microenvironment and gene expression further contribute to variations within the disease [1-3]. The current treatment regime for GBM includes surgical resection, radiotherapy and chemotherapy. The first line chemotherapeutic agent approved for human use in GBM is temozolomide (4-methyl-5-oxo-2,3,4,5,8-pentazabicyclo [4.3.0] nona-2,7,9-tiene-9-carboxamide) (TMZ). It belongs to the group of drugs known as antineoplastics. Although several other chemotherapeutic agents viz. bevacizumab, and a combination of procarbazine, lomustine and vincristine (PCV) have also been attempted but a recurrence of disease has been reported [4]. After the discovery of TMZ in 2005, there had been no significant developments in GBM pharmacotherapeutics and current survival rate is just 5.4%. TMZ resistance also limits the median survival of the patient. Factors like surgical non-removal of the tumor and blood brain barrier (BBB) further prevent the repurposing of drugs.

In order to overcome these issues, combination therapy with multiple drugs has been applied to treat drug resistant cancers. A few strategies have been developed to enhance the drug delivery efficacy. Recent advances in nanotechnology have made it plausible to synthesize materials that are biocompatible, biodegradable and possess a nano size. Further, they can be employed as carriers of drugs. These nanoparticles (NPs) offer several advantages in targeted drug delivery. NPs facilitate more effective cancer detection and treatment with minimum side effects on healthy cells. They restrict the non-specific absorption of the drug and prolonged biological half-life in systemic circulation. Recent studies have demonstrated the strength of nanoparticle-based delivery systems in cancer treatment [5]. For instance, silver nanoparticles (AgNPs) have exhibited significant anticancer properties. Non-cytotoxic doses of AgNPs are known to induce the expression of genes associated with impaired cell cycle progression, DNA damage and apoptosis in human cells [6]. Furthermore, experimental evidence shows that titanium dioxide nanoparticles (TiO₂NPs) too, showed anticancer properties by down-regulating genes in T98G human glioblastoma cells [7]. TiO₂NPs can be genotoxic over a range of concentrations without being cytotoxic [8].

Several studies conducted so far have emphasized upon the efficacy of anticancer drugs against GBM using *in vitro* models. However, certain studies on *in vivo* and *in ovo* models are also available [9]. These *in vitro* and *in vivo* studies have favored the employment of NPs in cancer therapy. Enhancing the sensitivity of TMZ by non-cytotoxic doses of suitable NPs thus appears to be a preferred strategy in the treatment of GBM. Given the promising characters of AgNPs and TiO₂NPs concerning their utilization in anticancer therapy, the aim of the present study was to demonstrate the modulation of cytotoxic effects of TMZ, if any, by AgNPs or TiO₂NPs. It is hypothesized that a combined drug and NP therapy might be helpful in the treatment of human GBM.

Materials and Methods

Reagents and chemicals

Temozolomide (temodar), titanium dioxide nano powder and dimethyl sulfoxide were purchased from Sigma - Aldrich Chemical Company, Missouri (USA), while silver nanoparticles were synthesized in the laboratory following the method of Mavani and Shah (2013) [10]. In addition, 3-(4,5-dimethylthiazol-2-yl)-2,5-diphenyl tetrazolium bromide (MTT), trypan blue and minimum essential medium were purchased from Himedia Laboratories Pvt Ltd. Mumbai, India. FBS was procured from Gibco (Montana, USA).

Cell line and culture conditions

Human GBM cell line - U87MG was supplied by National Centre for Cell Science, Pune (India). Cells were maintained in the presence of glutamine and non-essential amino acids (NEAA) in minimum essential medium (MEM) supplemented with 10% fetal bovine serum. Cells were microscopically checked every day to ensure their growth and viability. Cultures were incubated at 37°C and equilibrated in 5% CO₂ atmosphere as described by ATCC.

Synthesis of AgNPs

AgNPs were synthesized following the method suggested by Mavani and Shah (2013) [10]. Briefly, sodium borohydride was used to reduce silver nitrate. 10 ml of ice cold reducing agent was stirred for 20 minutes on a magnetic stirrer and 2 ml of mixed silver nitrate was added 1 drop per second and the reaction was stopped. By mixing both the solutions silver ions were reduced and clustered to form mono-dispersed nanoparticles. The solution was lyophilized using a lyophilizer (Labconco, Missouri, USA).

Characterization of nanoparticles

Standard methods viz. high resolution transmission electron microscopy (HRTEM), field emission scanning electron microscopy (FESEM), zeta potential measurement and energy dispersive x-ray analysis (EDAX) were employed to characterize silver and titanium nanoparticles. The topographic images of NPs were captured by FESEM through SU 8010 with EDS (Hitachi, Japan). HRTEM was performed employing H-7500 electron microscope (Hitachi, Japan). The zeta potential of silver and titanium nanoparticles was determined by a ZETASIZER (Anton Paar, India). Energy dispersive x-ray diffraction of the NPs was monitored using X-ray diffraction technique (Panalytical, Xpert pro, The Netherlands). The particle complexes were scanned in the 2 θ ranges 15 to 7000C range in continuous scan mode. All these observations were made at Sophisticated Analytical Instrumentation Facility (SAIF) and Central Instrumentation Facility (CIL) of Panjab University, Chandigarh (India).

Fourier transform infra red spectroscopy (FTIR) was employed to determine the high resolution spectrum of silver and titanium nanoparticles. The dried powder(s) of the NPs were mixed with potassium bromide and spectral analysis was monitored in the range of 400-4000 cm^{-1} at a resolution of 4 cm^{-1} . The interferograms provided information on the functional groups present in the nanoparticles. The Thermo NICOLET-IS-50 spectrophotometer was used for recording the present data. These observations were made at Central Research Facility of Indian Institute of Technology, New Delhi.

Determination of IC₅₀

IC₅₀ (half maximal inhibitory concentration) values for TMZ, AgNPs, and TiO₂NPs against GBM were determined following the OECD guidelines [11]. Briefly, 2×10^4 cells were grown in each well of a 96 well plate in 100 μl media. After 24h, when cells adhered to the surface of the well plate, the media was removed and the wells were rinsed with 200 μl of PBS and extracted with pasteur pipette. GBM cells were exposed to these agents at different concentrations ranging from 200 μM to 600 μM of AgNPs, 12.5 μM to 100.12 μM of TiO₂NPs and 200 μM to 600 μM of TMZ with MEM for 24h at 37°C in a 5% CO₂ atmosphere. The NPs were solved in the growth medium because of their easy suspension. All the experiments were performed in triplicates. The control wells contained 200 μl of the growth medium only. Percent mortality in GBM cells was calculated comparing the formazan formation in treated cells against the untreated ones. Mortality curves were plotted against the concentration in a logarithmic scale and IC₅₀ was calculated through four parameter logistic (4PL) regression model. Following equation described the curves:

$$Y = ax + b$$

Where y is the mortality percentage and x is the concentration. The four parameters tested included-minimum value (0 dose), maximum value (infinite dose), the point of inflection and Hill's slope of the curve. The data was analyzed by ANOVA with a 95% confidence interval ($p < 0.05$) followed by Tukey's post hoc test.

Trypan blue dye exclusion assay

The trypan blue dye exclusion assay was performed following the method described by Strober [12]. Briefly, 2×10^5 cells were seeded in a 12 well plate and allowed to adhere for 24h at required conditions. After 24h, cells were exposed to different treatments viz. TMZ,

TMZ+AgNPs and TMZ+TiO₂NPs and incubated at 37°C at 5% CO₂ atmosphere for 24h. Thereafter, media was removed from the wells and cells were trypsinized and cell suspension were mixed with 0.4% trypan blue solution at a ratio of 1:1 and incubated at room temperature for 15 minutes. The dead and live cells were counted using an automated cell counter (Thermofisher Scientific, USA).

MTT cell viability test

The MTT (3-(4,5-dimethyl-2-thiazolyl)-2,5 diphenyltetrazolium bromide) assay was used to record cell viability [13,14]. The effect of TMZ alone, TMZ+AgNPs and TMZ+TiO₂NPs were evaluated through MTT assay. GBM cells (2x10⁵ cells/ml in 100 µl of culture medium) were seeded out into culture plates. After 24 h of seeding, cells were incubated with selected concentration(s) 150 µM, 220 µM and 280 µM of TMZ alone and with NPs (140 µM, 175 µM and 250 µM for AgNPs and 12.5 µM, 18.7 µM and 25 µM for TiO₂NPs) at 37°C for 24h. After treatment, 25 µl of 5 mg/ml MTT was added to each well and incubated for 4h at 37°C. MTT solution was removed and remaining insoluble formazan crystals were dissolved in 150 µl of DMSO. Absorbance was measured at 570 nm using a microplate reader (Electronics Corporation, Hyderabad, India).

The following formula was applied to calculate the cell viability:

$$\text{Cell viability (\%)} = \frac{\text{OD value of treatment}}{\text{OD value of control}} \times 100$$
$$\% \text{ Inhibition} = 100 - \text{cell viability (\%)}$$

Cell proliferation assay

The proliferation of GBM cells under the influence of TMZ alone and in combination with AgNPs and TiO₂NPs was assayed by MTT cell proliferation assay as described by Mosmann [14]. After 24h incubation of GBM cells with TMZ, TMZ+AgNPs and TMZ+TiO₂NPs, 25 µl of the MTT reagent was added to the medium and incubated under standard culture conditions for 4h. The images of GBM cells before and after dosing were captured using a phase contrast microscope (Nikon, Japan).

Estimation of malondialdehyde (TBARS)

Malondialdehyde (MDA) in the cell lysate was estimated following the method of Jordan and Schenkman [15]. Absorbance was recorded at 532 nm using a spectrophotometer (Systronics, India). 1,1',3,3' tetramethoxypropane (Sigma) was used as the standard. Total proteins were determined following Bradford method [16]. Bovine serum albumin (BSA) was used as the standard.

Estimation of reduced glutathione (GSH)

GSH was determined using Ellmans' reagent [17]. An aliquot was added to phosphate buffer (pH 7.4) and 5',5' dithiobis 2-nitrobenzoic acid. Absorbance was recorded at 412 nm using a spectrophotometer (Systronics, India).

Statistical analyses

Statistical analyses were carried out using SPSS (version 20) software (SPSS Inc. Chicago, IL, USA). The results are presented as means ± S.E.

Results

FESEM and HRTEM images

The shape of nanoparticles was determined by FESEM. AgNPs exhibited a spherical shape. These particles formed agglomeration (Figure 1). Whereas, the shape of TiO₂NPs was found to be irregular. Clusters of NPs were also observed (Figure 2). The size of nanoparticles was

calculated by Debye-Scherrer equation. Mean size of AgNPs was found to be 72.005 nm, whereas, the mean size of TiO₂NPs was registered as 22.30 nm. The results obtained through FESEM were confirmed through HRTEM observations (Figure 3 and 4).

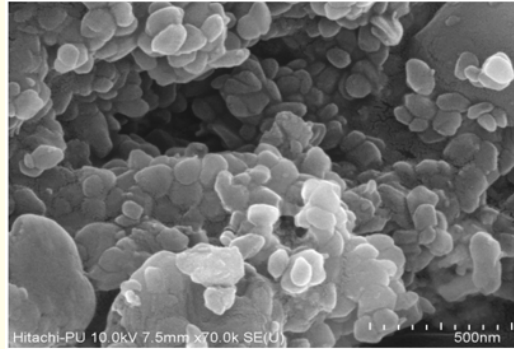


Figure 1: FESEM image of silver nanoparticles.

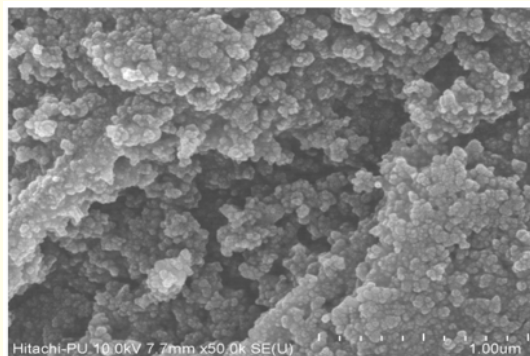


Figure 2: FESEM image of titanium nanoparticles.

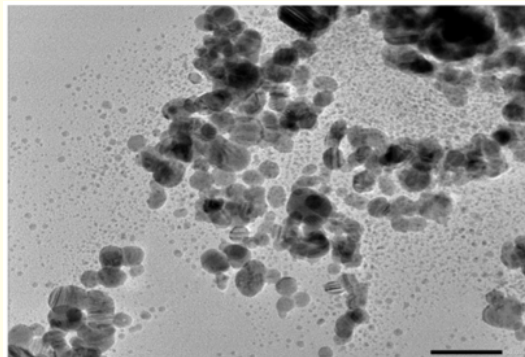


Figure 3: HRTEM image of silver nanoparticles (scale - 50 nm).

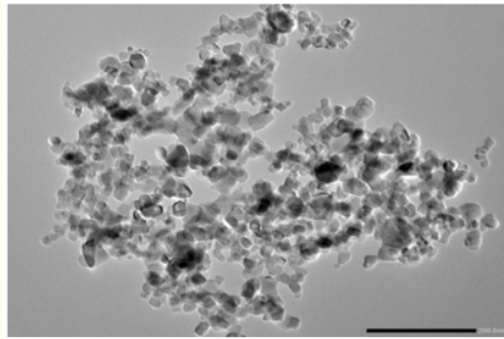


Figure 4: HRTEM image of titanium nanoparticles (Scale- 200 nm).

Zeta potential measurements and particle size distribution

The zeta potential of AgNPs exhibited stability. It was recorded as -27.3 mV. Whereas, the zeta potential of TiO₂NPs averages -13 mV (Figure 5 and 6). AgNPs showed a wide particle size distribution while particle size distribution of TiO₂NPs was narrow but uniform (Figure 7 and 8).

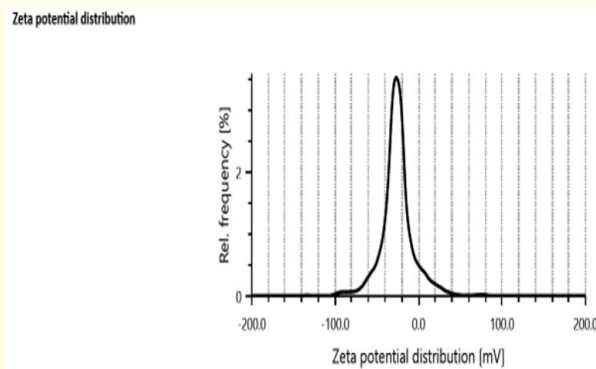


Figure 5: Zeta Potential of silver nanoparticles.

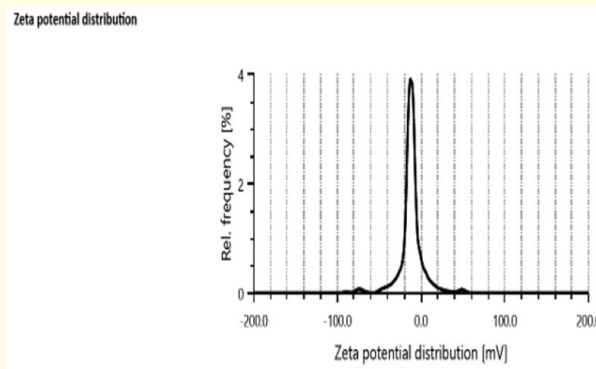


Figure 6: Zeta Potential of titanium nanoparticles.

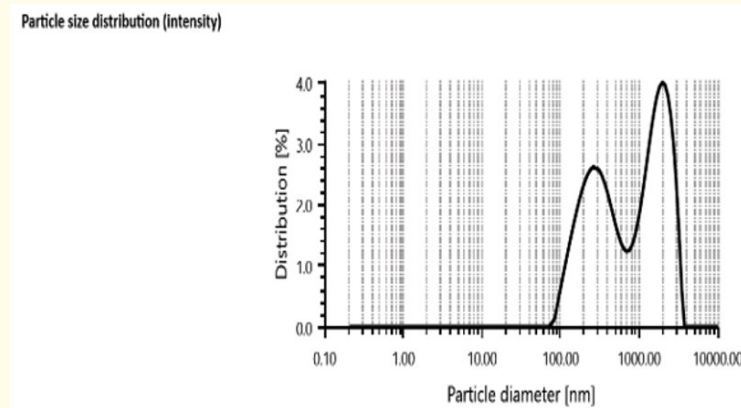


Figure 7: Particle size distribution of silver nanoparticles.

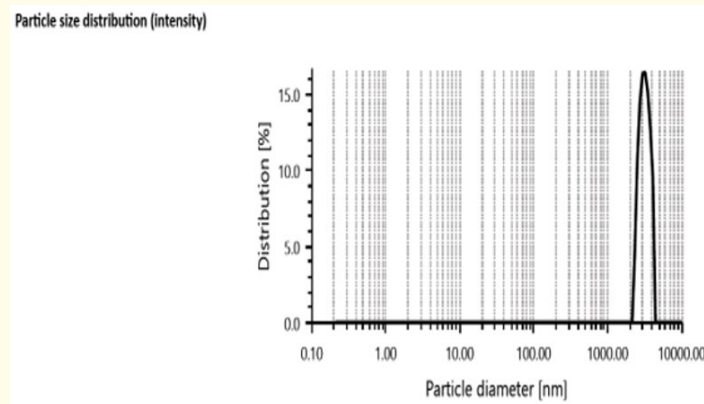


Figure 8: Particle Size distribution of titanium nanoparticles.

Energy dispersive x-ray analysis (EDAX) of AgNPs and TiO₂NPs

EDAX was used to find out the elemental composition in the reaction mixture. EDAX of AgNPs revealed the percentage i.e. 41.06% of pure silver in the NPs employed in present study. It comprised silver as the major element as compared to sodium and carbon (Figure 9). Similarly the samples of TiO₂NPs were also analyzed for the concentration of titanium. These particles exhibited 48.90% of titanium in the samples as compared to carbon and oxygen (Figure 10).

X-ray diffraction (XRD)

The structural analysis of AgNPs and TiO₂NPs was performed by X-ray diffraction. The X-ray diffraction patterns showed peaks of silver nitrate and titanium dioxide along with the peaks of nano silver and nano titanium. The X-ray diffraction pattern for AgNPs indicated a peak pattern at 2 theta/Degree, i.e. 31° angle (Figure 11). Whereas the peak pattern for TiO₂NPs was noticed at 26° angle (Figure 12). The main crystalline phases in AgNPs and TiO₂NPs were silver and titanium free from other impure phases.

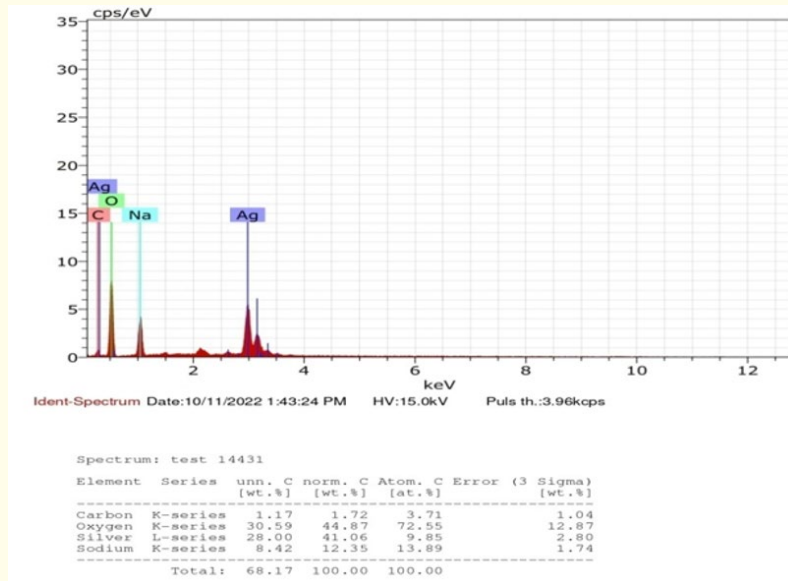


Figure 9: Energy dispersive x-ray analysis (EDAX) of silver nanoparticles.

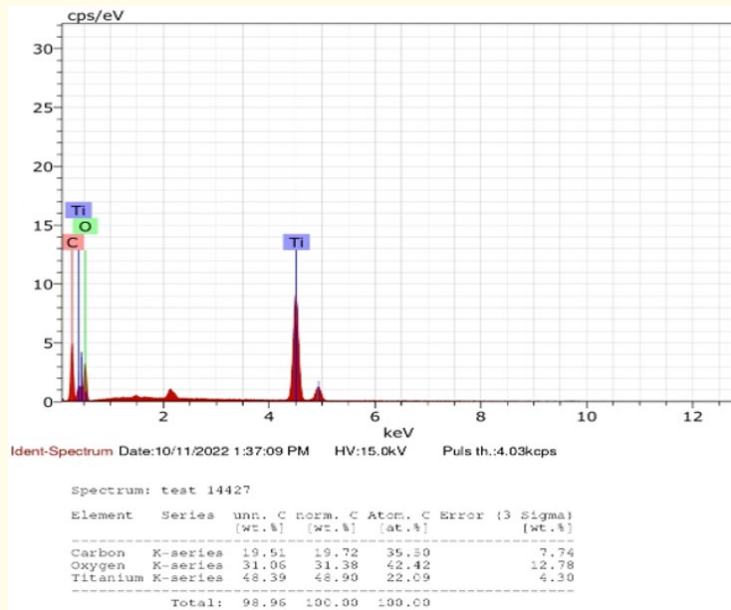


Figure 10: Energy dispersive x-ray analysis (EDAX) of titanium nanoparticles.

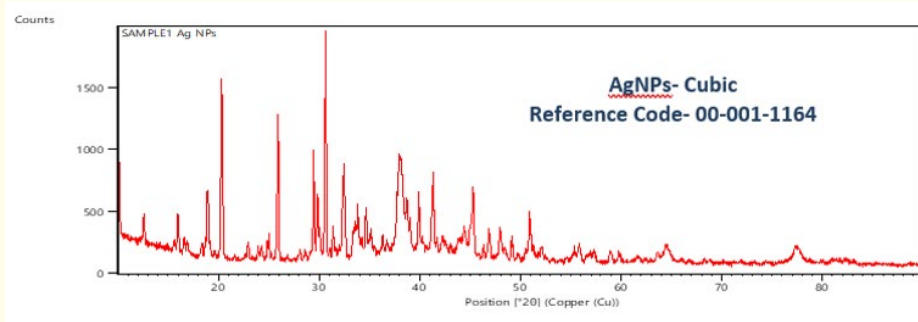


Figure 11: XRD pattern of silver nanoparticles.

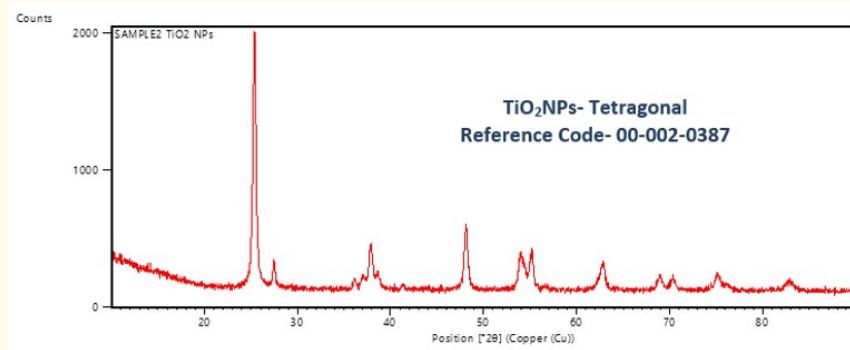


Figure 12: XRD pattern of titanium nanoparticles.

FTIR

FTIR analysis of AgNPs

FTIR spectrum of AgNPs is exhibited by figure 13. The absorption bands at 3498.65 cm^{-1} are associated with NH (amide) and OH (alcohol) stretching. The peaks between 2000 - 1600 are associated with carbonyl and CH groups. It has been confirmed that carbonyl groups from proteins and amino acids have strong affinity with NPs and act as capping or stabilizing agents.

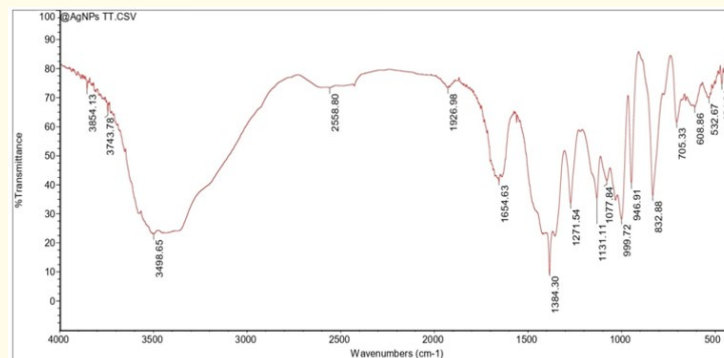


Figure 13: FTIR spectra of silver nanoparticles.

FTIR analysis of TiO₂NPs

FTIR spectrum of TiO₂NPs is shown by figure 14. The broadest band was observed at 3425.92 cm⁻¹ corresponding to the hydroxyl group. The peaks 1383.85 - 1700.94 cm⁻¹ were associated with C=O and C=N stretching. These peaks indicate hydrogen binding nature of NPs.

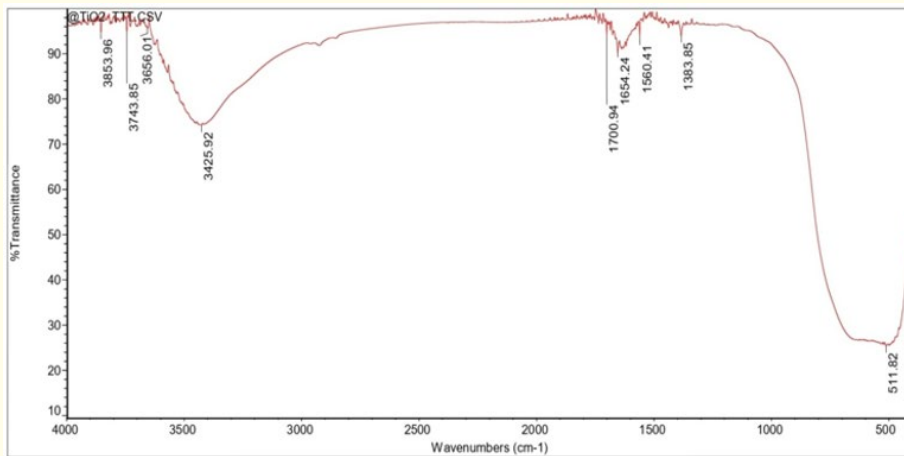


Figure 14: FTIR Spectra of titanium nanoparticles.

IC50 values

The half maximal inhibitory concentration (IC₅₀) values for TMZ, AgNPs and TiO₂NPs at 24 hours were calculated to be 530 μM, 526.26 μM and 58.82 μM respectively using GraphPad Prism 5 (Graphpad Software Inc, San Diego, USA).

| Drug/Nanoparticles | IC ₅₀ (24 hrs) |
|----------------------|---------------------------|
| TMZ | 530.9 μM |
| AgNPs | 526.26 μM |
| TiO ₂ NPs | 58.82 μM |

Table 1: IC₅₀ values for temozolomide, silver nanoparticles (AgNPs) and titanium dioxide nanoparticles (TiO₂NPs) in the glioblastoma multiforme U87MG cell line at 24 hours.

Cell viability

U87MG GBM cells showed 95.50% survival in the culture medium alone. However, their survival rate was inhibited by TMZ. A linear dose-response relationship between increasing concentration of TMZ and percent viability of GBM cells was registered (Figure 15). Inhibition was concentration dependent. Maximum inhibition was recorded at 280µM while minimum effect was recorded at 150 µM.

TiO₂NPS also influenced the viability of U87MG cells in a dose dependent manner. A higher dose of 25 µM significantly inhibited the cell survival whereas minimum effect was expressed at 12.5 µM (Figure 15).

Dose dependent variations were noticed after incubation of cells with AgNPs for 24h. Maximum inhibition was registered at 250 µM whereas minimum effect was recorded at 140 µM (Figure 15).

Combined effects of TMZ+AgNPs and TMZ+TiO₂NPs on cell viability were also determined. Amongst TMZ+AgNPs treated cells, maximum inhibition was recorded at a concentration of 280 µM+140 µM. Whereas amongst TMZ+TiO₂NPs treated cells maximum inhibition was registered at the concentration of 280 µM+25 µM. Better effects of AgNPs+TMZ were noticed than in the cells treated with TiO₂NPs+TMZ (Figure 15).

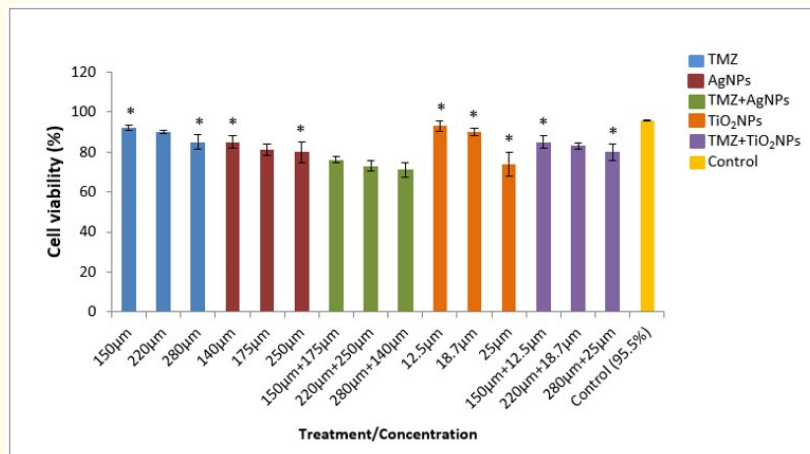


Figure 15: Effect of TMZ, AgNPs and TiO₂NPs on cell viability of U87MG cells at different concentrations. Values are expressed as mean ± SE (n = 3). *p < 0.05 vs control.

MTT assay

This assay was employed to determine the metabolic activity of GBM cells. The assay is based on the ability of NADPH dependent cellular oxido-reductase enzymes to reduce the tetrazolium dye - MTT to its insoluble formazan. The results show dose dependent effects of TMZ, AgNPs and TiO₂NPs on viability of GBM cells. Percentage of viability was very high in GBM cells in present culture conditions. However, the viability decreased in a dose dependent manner in TMZ treated GBM cells. Maximum inhibition in cell viability was recorded at a concentration of 280µM (Figure 16). In AgNPs treated cells also maximum inhibition was recorded at 250µM. In TMZ+AgNPs treated cells also, maximum inhibition was recorded at 280 µM+140 µM. Amongst TiO₂NP treated cells, maximum inhibition was recorded at the highest dose of 25µM. However, in TMZ+TiO₂NPs treated group, maximum inhibition was recorded at a concentration of 220 µM+18.7 µM (Figure 16).

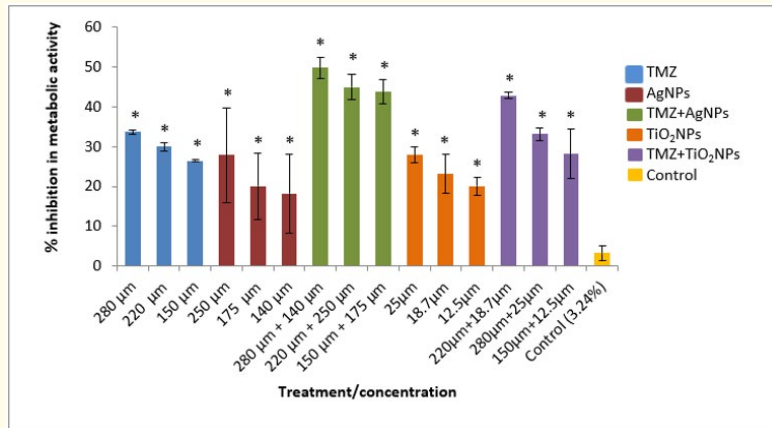
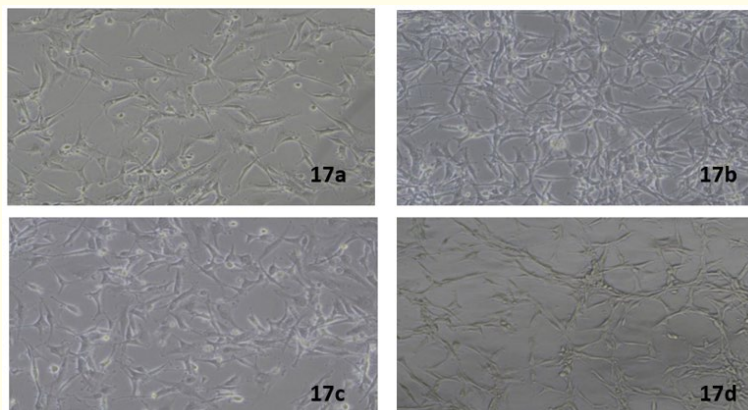


Figure 16: Effect of TMZ, AgNPs, TiO₂NPs, TMZ+AgNPs and TMZ+TiO₂NPs on metabolic activity (MTT) of GBM. Values are expressed as mean \pm SE (n=3). *p < 0.05 vs control.

Cell proliferation

Cell proliferation refers to an increase in the number of cells as a function of time without an increase in the size of cells. Present studies on cell proliferation were made using a phase contrast microscope (Nikon, Japan). A comparison of time dependent studies were made between 0h and 24h of incubation at 37°C with TMZ and NPs. Results on control/untreated GBM cell showed an increase in cell population after 24h incubation (Figure 17a and 17b). The effects of TMZ alone on cell proliferation are exhibited by figure 17c and 17d. A marked decrease in cell proliferation was noticed. AgNPs alone also inhibited cell proliferation (Figure 17e and 17f). However, GBM cell proliferation, further decreased in TMZ+AgNPs treated cells (Figure 17g and 17h). TiO₂NPs did inhibit the proliferation of GBM cells (Figure 17i and 17j). However, further decrease in the number of cells was recorded in TMZ + TiO₂NPs treated cells (Figure 17k and 17l).



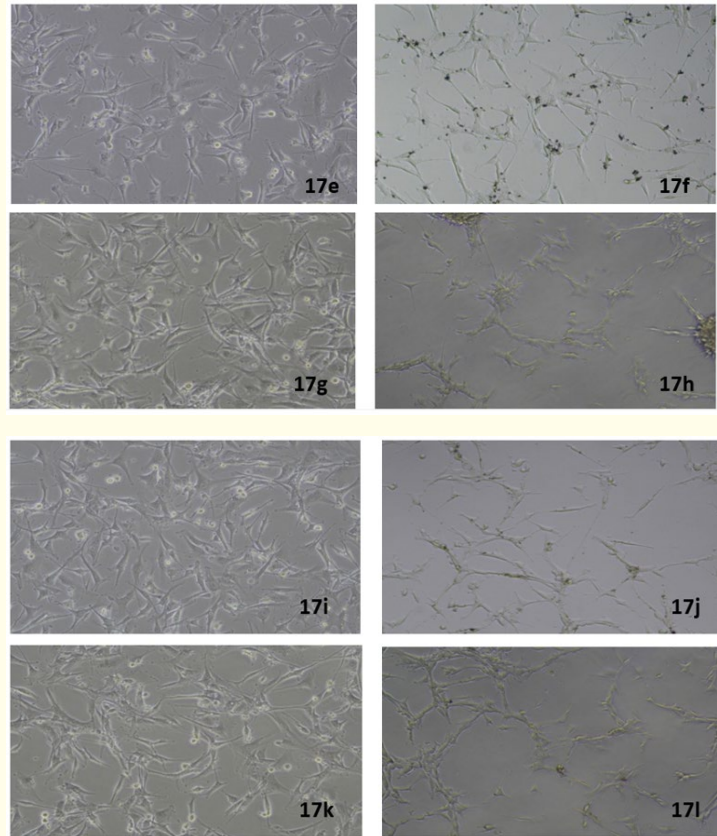


Figure 17: The cytotoxic effect of TMZ alone and in combination with AgNPs & TiO₂NPs is exhibited by figure 17a-17l. The comparison of effect was made between 0h and 24h of incubation at a selected concentration of TMZ, AgNPs and TiO₂NPs. All images were captured at a magnification of 10X.

17a: Control 0 hr, 17b: Control 24 hr, 17c: TMZ 0 hr (220 μM), 17d: TMZ 24 hr (220 μM), 17e: AgNPs 0 hr (250 μM), 17f: AgNPs 24 hr (250 μM), 17g: TMZ+AgNPs 0 hr (220 μM+250 micron (mu)), 17h: TMZ+AgNPs 24 hr (220 μM+250 μM), 17i: TiO₂NPs 0 hr (18.7 uM), 17j: TiO₂NPs 24 hr (18.7 micron (mu)), 17k: TMZ+TiO₂NPs 0 hr (220 μM+18.7 micron (mu)), 17l: TMZ+TiO₂NPs 24 hr (220 μM+18.7 micron (mu)).

TBARS

These results showed a dose dependent effect of TMZ on the generation of reactive species in GBM cells (Figure 18a). However, TMZ in combination with silver and titanium nanoparticles increased the generation of TBARS (Figure 18c and 18e). Nonetheless, nanoparticles of silver and titanium alone could induce the generation of TBARS in GBM cells (Figure 18b and 18d).

GSH

TMZ initially at a low dose (150 μM) enhanced the synthesis of GSH in GBM cells. However, its inhibition was recorded at higher doses of 220 μM and 280 μM (Figure 19a). A combined treatment of TMZ and AgNPs did inhibited GSH synthesis in a dose dependent manner (Figure 19c). Similar trend was recorded in GBM cells treated with TMZ and TiO₂NPs (Figure 19e). Treatment(s) of GBM cells with AgNPs and TiO₂NPs only, enhanced GSH values at low doses but decreased the values at higher doses (Figure 19b and 19d).

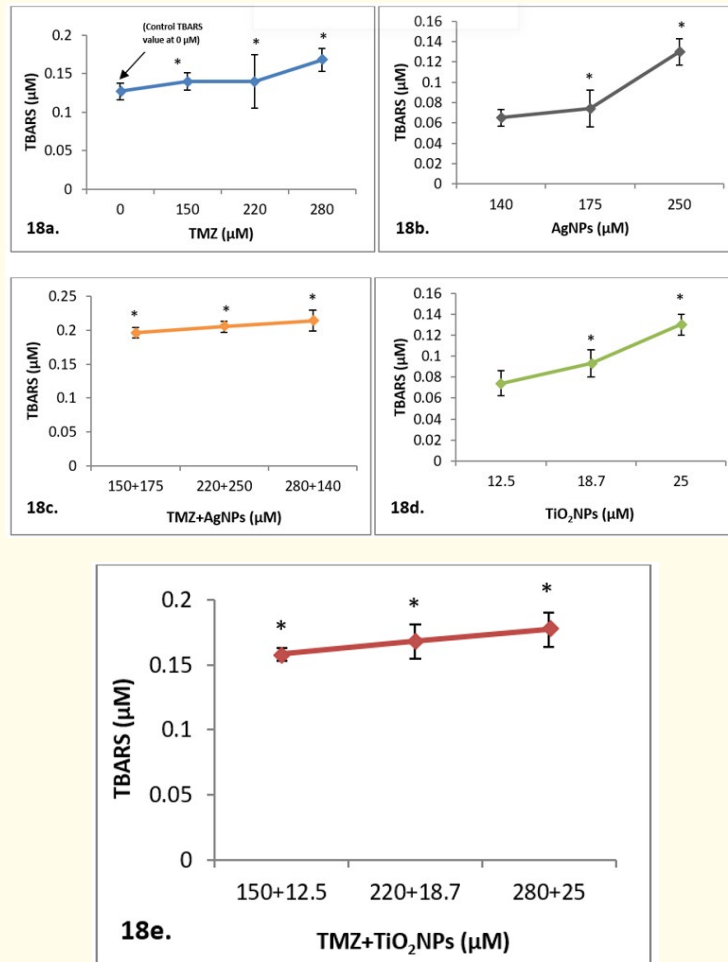


Figure 18: 18a: TMZ increases the formation of TBARS in GBM cells in a dose dependent manner.

18b: AgNPs enhance the production of TBARS in GBM cells.

18c: TMZ and AgNPs together show an additive effect on TBARS in GBM cells.

18d: TiO₂NPs increase TBARS in GBM cells in a dose dependent manner.

18e: TMZ and TiO₂NPs together express an additive effect on the formation of TBARS. (Values are expressed as mean ± SE (n = 3).

*p < 0.05 vs control).

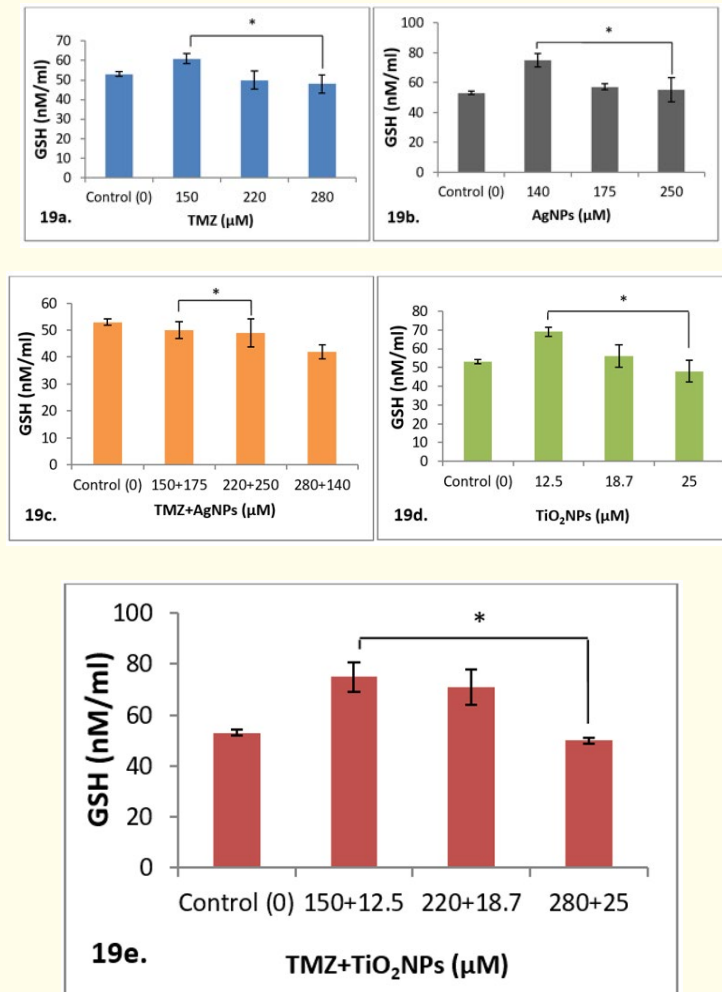


Figure 19: 19a: Increasing dose of TMZ reciprocates the decrease in GSH.

19b: AgNPs inhibit GSH in GBM at higher doses.

19c: TMZ+AgNPs expressed inhibition of GSH in GBM cells.

19d: Increasing doses of TiO₂NPs reciprocated with the decrease in GSH in GBM cells.

19e: GSH inhibition in GBM cells was witnessed at high dosage of TMZ+TiO₂NPs. (Values are expressed as mean ± SE (n = 3). *p < 0.05 vs control).

Discussion

Standard parameters employed to test the cytotoxicity of TMZ against GBM cells exhibited a dose dependent effect on cell viability, MTT assay, cell proliferation, lipid peroxidation and oxidative stress. The chemotherapeutic potential of TMZ in the treatment of primary and recurrent GBM has been established now [18]. TMZ (4-methyl-5-oxo-2, 3,4,6,8 pentazabicyclo [4.3.0] nona-2,7,9-tiene-9 carboxamide)

is a small pro-drug, with a molecular weight of 194.15. It possesses unique pharmacokinetic properties that allow its entry into the cells in a dose dependent manner. Its immense potential to kill GBM is attributed to its metabolite, a reactive species 5-(3-methyl-1-triazeno) imidazole-4-carboxamide (MTIC). It generates an active methyl group that reacts with DNA bases of guanine at O⁶ position [19]. O⁶ methylguanine leads to DNA mismatch repair that causes double strand breaks and apoptosis [20]. Hence, it is believed that generation of O⁶ methyl guanine and a functional DNA mismatch repair pathway manifests the cytotoxicity of TMZ. In non human primate models, the peak levels of drug have been found to be 104 ± 3 µM in plasma. Present results show the maximum cytotoxicity occurred at 280 µM of TMZ while minimum effects were registered at 150 µM in human GBM cells.

Available literature show that a few strategies have been considered to improve therapeutic efficacy of TMZ via inhibition of O⁶-methylguanine-DNA-methyltransferase (MGMT), a DNA repair enzyme, that may counteract TMZ induced DNA alkylation [21]. Modulation of TMZ induced cytotoxicity by AgNPs in GBM cells was witnessed during present investigations. Previous studies on cytotoxicity of AgNPs on glioblastoma and breast cancer cells [22,23] support present results. Data on MTT assay obtained on A549 and MCF cells after treatment with AgNPs have also confirmed its anticancer properties [24]. Silver nanoparticles are known to enhance the sensitivity of TMZ on human GBM cells [25]. However, the mechanism of modulation remains so far unknown. Silver is released from AgNPs after its uptake by GBM that interferes with intracellular repair processes. One amongst these processes might be the inhibition of MGMT. Protective effects of AgNPs against cancer have been recently debated [26]. AgNPs might enter the cancer cells through an enhanced permeability and retention (EPR) mechanism [27]. Secondly, bioaccumulation through endocytic mechanisms and consequent generation of ROS might induce cytotoxicity [28]. Oxidative stress induced by silver ions in *in vivo* systems reported earlier [29,30] further support ROS/oxidative stress mediated mechanism of toxicity of AgNPs in GBM cells.

Another set of observations did confirm the cytotoxicity of TiO₂NPs in GBM cells. Toxic effects of TiO₂NPs have been studied in several *in vitro* systems viz. human liver and lung cancer cells [31-33]. They are known to inhibit proliferation of glial U373 cells also [34]. NPs are internalized in nerve cells through clathrin endocytosis, transported to lysosomes where they activate lysosomal proteases [35]. TiO₂NPs are also known to generate ROS in human keratinocyte HaCaT cells [36] and immortalized brain microglia [37]. Small sized NPs produce greater genotoxicity reciprocating to increased generation of ROS [38]. Thus present results on cytotoxicity of TiO₂NPs are also attributed to ROS.

During present investigations, combined effects of TMZ+AgNPs were found to be more cytotoxic than those of TMZ+TiO₂NPs. ROS and oxidative stress seemingly explain the mechanism of their cytotoxicity. Synergistic effect of TMZ+AgNPs may be linked to inhibition/degradation of MGMT by AgNPs and related mechanisms. AgNPs are known to cause a significant decrease in DNA methylation in mouse breast cancer cells [39]. Silver nanoparticle induced DNA hypomethylation through proteasome-mediated degradation of methyltransferase 1 in A549 alveolar epithelial cells has been suggested [40]. However, effects of TMZ+TiO₂NPs on GBM cell were found to be less cytotoxic than AgNPs+TMZ. Nevertheless, TiO₂NPs are also known to cause DNA hypomethylation in human peripheral blood mononuclear cells in a dose dependent manner [41]. Pogribna studied the effect of TiO₂NPs on DNA methylation in multiple human cell lines and suggested the involvement of this epigenetic mechanism in the toxicity of TiO₂NPs [42]. Nevertheless, Studies focusing on the effects of nanoparticles on MGMT are very limited and further investigations are needed to support present results.

In general, size, shape and other physiochemical properties of NPs influence their chemotherapeutic effects. Present results showed that there was a relationship between the % GBM cell viability and % GBM cell inhibition with the different concentrations of TMZ and AgNPs and TiO₂NPs. The same relationship has been reported for A549 and MCF7 cell lines [43]. Their effects on cell viability, metabolic activity and proliferation may be attributed to a phenomenon known as “nanomaterial induced endothelial cells leakiness” (NanoEL). It is assumed that by changing the nanoscale dimensions of NPs, the movement of these NPs inside the nanosized gaps between microvascular capillary endothelial cells and dislocated protein connections that embrace the neighboring cells might be altered. In brief, present results confirm that a combined therapy of TMZ and nanoparticles offers better antitumor results than TMZ alone. Additional *in vivo* studies are expected to confirm their suitability in the treatment of glioblastoma multiforme.

Acknowledgement

The authors express their sincere gratitude to the Director, Sophisticated Analytical Instrumentation Facility and Central Instrumentation Laboratory, Punjab University, Chandigarh and Central Research Facility, IIT Delhi for helping in the characterization of nanoparticles.

Funding Support

This work was supported by the University Grants Commission (India). Research Grant Scheme with Project Code: (636/(CSIR-UGC NET DEC. 2017).

Data Availability Statement

The data supporting the findings of this study are available from the corresponding authors upon request.

Declaration of Competing Interests

Authors declare no conflict of interest.

Bibliography

1. Verhaak RGW., *et al.* "Integrated genomic analysis identifies clinically relevant subtypes of glioblastoma characterized by abnormalities in PGDFRA, IDH1, EGFR and NF1". *Cancer Cell* 17.1 (2010): 98-110.
2. Alcantara Llaguno SR., *et al.* "Adult lineage-restricted CNS progenitors specify distinct glioblastoma subtypes". *Cancer Cell* 28.4 (2015): 429-440.
3. Broekman ML., *et al.* "Multidimensional communication in the microenvirons of glioblastoma". *Nature Reviews Neurology* 14.8 (2018): 482-495.
4. Tan AC., *et al.* "Management of glioblastoma: State of the art and future directions". *CA: A Cancer Journal for Clinicians* 70.4 (2020): 299-312.
5. Peer D., *et al.* "Nanocarriers as an emerging platform for cancer therapy". *Nature Nanotechnology* 2 (2007): 751-760.
6. Asharani PV., *et al.* "Antiproliferative activity of silver nanoparticles". *BMC Cell Biology* 10 (2009): 65.
7. Fuster E., *et al.* "Titanium dioxide, but not zinc oxide nanoparticles cause severe transcriptomic alterations in T98G human glioblastoma cells". *International Journal of Molecular Sciences* 22.4 (2021): 2084.
8. Osman IF., *et al.* "Genotoxicity and cytotoxicity of zinc oxide and titanium oxide in HEP-2 cells". *Nanomedicine (London)* 5.8 (2010): 1193-1203.
9. Ribatti D. "The chick embryo chorioallantoic membrane as a model for tumor biology". *Experimental Cell Research* 328.2 (2014): 314-324.
10. Mavani K and Shah M. "Synthesis of silver nanoparticles by using sodium borohydride as a reducing agent". *International Journal of Engineering Research & Technology (IJERT)* 2.3 (2013).
11. OECD, OECD series on testing and assessment 2014. Number 211. Guidance document for describing non-guideline *in vitro* test methods. ENV/JM/MONO(2014)35.
12. Strober W. "Trypan blue exclusion test of cell viability". *Current Protocols in Immunology* Appendix 3 (2001): Appendix 3B.

13. Plumb JA. "Cell sensitivity assays: the MTT assay". *Methods in Molecular Medicine* 88 (2004): 165-169.
14. Mosmann T. "Rapid colorimetric assay for cellular growth and survival: application to proliferation and cytotoxicity assays". *Journal of Immunological Methods* 65.1-2 (1983): 55-63.
15. Jordan RA and Schenkman JB. "Relationship between malondialdehyde production and arachidonate consumption during NADPH-supported microsomal lipid peroxidation". *Biochemical Pharmacology* 31.7 (1982): 1393-1400.
16. Kruger NJ. "The Bradford method for protein quantitation". *The protein protocols handbook* (2009): 17-24.
17. Ellman GL. "Tissue sulfhydryl groups". *Archives of Biochemistry and Biophysics* 82.1 (1959): 70-77.
18. Nam JY and de Groot JF. "Treatment of glioblastoma". *Journal of Oncology Practice* 13.10 (2017): 629-638.
19. Denny BJ, et al. "NMR and molecular modeling investigation of the mechanism of activation of the anti-tumor drug temozolomide and its interaction with DNA". *Biochemistry* 33.31 (1994): 9045-9051.
20. Roos WP, et al. "Apoptosis in malignant glioma cells triggered by the telozolomide induced DNA lesion O6 methyl guanine". *Oncogene* 26.2 (2007): 186-197.
21. Fan CH, et al. "O6-methylguanine DNA methyltransferase as a promising target for the treatment of temozolomide-resistant gliomas". *Cell Death and Disease* 4.10 (2013): e876.
22. Jeyraj M, et al. "Biogenic silver nanoparticles for cancer treatment: an experimental report". *Colloids and Surfaces B: Biointerfaces* 106 (2013): 86-92.
23. Locatelli E, et al. "Targeted delivery of silver nanoparticles and alisertib: in vitro and in vivo synergistic effect against glioblastoma". *Nanomedicine (London)* 9.6 (2014): 839-849.
24. Kundu M, et al. "pH responsive and targeted delivery of curcumin via phenylboronic acid-functionalized ZnO nanoparticles for breast cancer therapy". *Journal of Advanced Research* 18 (2019): 161-172.
25. Liang P, et al. "Silver nanoparticles enhance the sensitivity of temozolomide on human glioma cells". *Oncotarget* 8.5 (2017): 7533-7539.
26. Kovacs D, et al. "Cancer therapy by silver nanoparticles: fiction or reality". *International Journal of Molecular Sciences* 23.2 (2022): 839-865.
27. Kalyane D, et al. "Employment of enhanced permeability and retention effect (EPR): Nanoparticle based precision tools for targeting of therapeutic and diagnostic agent in cancer". *Materials Science and Engineering* 98 (2019): 1252-1276.
28. Hasse H, et al. "Impact of silver nanoparticles and silver ions on innate immune cells". *Journal of Biomedical Nanotechnology* 10.6 (2014): 1146-1156.
29. Rana SVS. "Metals and apoptosis: recent developments". *Journal of Trace Elements in Medicine and Biology* 22.4 (2008): 262-284.
30. Yu Z, et al. "Reactive oxygen species - related nanoparticle toxicity in the biomedical field". *Nanoscale Research Letters* 15.1 (2020): 115-129.
31. Shukla RK, et al. "TiO₂ nanoparticles induce oxidative DNA damage and apoptosis in human liver cell". *Nanotoxicology* 7.1 (2013): 48-60.

32. Wang Y, *et al.* "Cytotoxicity, DNA damage and apoptosis induced by titanium dioxide nanoparticles in human non-small lung cancer A549 cells". *Environmental Science and Pollution Research International* 22.7 (2014): 5519-5530.
33. Brandao F, *et al.* "Genotoxicity of TiO₂ nanoparticles in four different human cell lines (A549, HEPG2, A172 and SH-SY5Y)". *Nanomaterials* 10.3 (2020): 412.
34. Marquez-Ramirez SG, *et al.* "Titanium dioxide nanoparticles inhibit proliferation and induce morphological changes and apoptosis in glial cells". *Toxicology* 302.2-3 (2012): 146-156.
35. Kenzaoui BH, *et al.* "Induction of oxidative stress, lysosome activation and autophagy by nanoparticles in human brain derived endothelial cells". *Biochemical Journal* 441.3 (2012): 813-821.
36. Xue C, *et al.* "Nano titanium dioxide induces the generation of ROS and potential damage in HaCaT cells under UVA irradiation". *Journal of Nanoscience and Nanotechnology* 10.12 (2010): 8500-8507.
37. Long TC, *et al.* "Titanium dioxide (P25) produces reactive oxygen species in immortalized brain microglia (BV2): implications for nanoparticle toxicity". *Environmental Science and Technology* 40.14 (2006): 4346-4352.
38. Liao F, *et al.* "The size dependent genotoxic potential of titanium dioxide nanoparticles to endothelial cells". *Environmental Toxicology* 34.11 (2019): 1199-1207.
39. Brzoska K, *et al.* "Silver nanoparticles induced changes in DNA methylation and histone H3 methylation in a mouse model of breast cancer". *Materials (Basel)* 16.11 (2023): 4163.
40. Maki A, *et al.* "Silver nanoparticles induce DNA hypomethylation through proteasome mediated degradation of DNA methyltransferase 1". *Biological and Pharmaceutical Bulletin* 43.12 (2020): 1924-1930.
41. Malakootian M, *et al.* "Effect of titanium dioxide nanoparticles on DNA methylation of human peripheral blood mononuclear cells". *Toxicology Research* 10.5 (2021): 1045-1051.
42. Pogribna M, *et al.* "Effect of titanium dioxide nanoparticles on DNA methylation in multiple human cell lines". *Nanotoxicology* 14.4 (2020): 534-553.
43. Isakoff WH, *et al.* "Low-dose continuous 5-fluorouracil combined with leucovorin, nabpaclitaxel, oxaliplatin and bevacizumab for patients with advanced pancreatic cancer: a retrospective analysis". *Targeted Oncology* 13.4 (2018): 461-468.

Volume 12 Issue 9 September 2024

© All rights reserved by S V S Rana, *et al.*